J|A|C|S
ARTICLES
Published on Web 05/12/2006

Stepwise Cope Rearrangement of Cyclo-biphenalenyl via an Unusual Multicenter Covalent π-Bonded Intermediate

Jingsong Huang and Miklos Kertesz*

Contribution from the Department of Chemistry, Georgetown University, 37th and O Street, Washington, D.C. 20057-1227

Received January 19, 2006; E-mail: kertesz@georgetown.edu

Abstract: Multicenter covalent π-bonding between π-conjugated radicals has been recently recognized as a novel and important bonding interaction. The Cope rearrangement of cyclo-biphenalenyl **9** is studied by exploring its potential energy surface with density functional theory (DFT), and it is found that π-bonding plays a critical role in the rearrangement process. Affected by this, the rearrangement of **9** takes place by a stepwise mechanism through an unusual π-intermediate **10**, of C_{2h} symmetry, which can be characterized as a $2\times13\pi+2\times2\pi$ system. The π-intermediate has a long inter-phenalenyl distance of $R \approx 2.8$ Å, which is shorter than the sum of the van der Waals radii displaying multicenter covalent π-bonding between the two phenalenyl units. The energy of the π-intermediate **10** is higher than that of the σ-bonded reactant **9** by ~2 kcal/mol according to the employed spin-restricted DFT. NMR chemical shift calculations support the σ-bonded **9** as the global minimum. The calculated activation barrier of ~6 kcal/mol for the Cope rearrangement is consistent with the stepwise mechanism. A covalent π-bonding effect in the π-intermediate **10** is demonstrated indirectly by the shortening of inter-naphthalene distance of the dianion and dication of the cyclophane **14** compared to that of its neutral counterpart. The unusual π-bonded structure with a long inter-phenalenyl distance becomes the most stable structure for the ethano-bridged derivative **13**, which should have observable paramagnetism according to the calculated paramagnetic susceptibility.

Introduction

The Cope rearrangement of 1,5-hexadiene (**1**) is a symmetry-allowed [3,3]-sigmatropic reaction (Scheme 1).[1] The nature of its chair transition structure has been the subject of many experimental[2] and theoretical investigations.[3] It is now widely accepted[4] that this archetypal Cope rearrangement is concerted and proceeds via an aromatic chairlike C_{2h} transition structure **2**, which has an inter-allylic bond length of $R \approx 2.0$ Å.

The transition structure also contains contributions from the resonance structures of cyclohexane-1,4-diyl (**3**) and bis-allyl diradicals (**4**).[5] Density functional theory (DFT) studies show that substitutions with radical stabilizing groups at C2 and C5 of **1** can enhance the contribution from the resonance structure

Scheme 1. Cope Rearrangement of 1,5-Hexadiene (**1**)

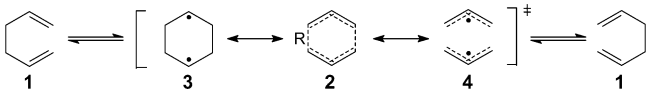

3, leading to transition structures with small R values down to 1.7 Å, while the substitutions at C1, C3, C4, and C6 can stabilize the contribution from the resonance structure **4**, leading to transition structures with large R values up to 2.6 Å.[5] The term "chameleonic" has been suggested to describe the variable transition structures with a wide range of R values from 1.7 to 2.6 Å.[6] In some substitution cases, the rearrangement could be stepwise, proceeding through a diradicaloid intermediate with a short R around 1.6 Å,[5,7] and yet *an intermediate with a relatively long R value (e.g., R > 2.6 Å) has never been found*.

The transition structures depicted above can be recognized as two interacting allyl radicals,[8] the simplest odd alternant hydrocarbon. Another odd alternant hydrocarbon analogous to the allyl radical is the phenalenyl radical (**5**). Both the allyl radical and **5** are stable radicals because the unpaired electrons are delocalized over the singly occupied molecular orbitals (SOMOs). The stability of **5** allows it to be observed by electron spin resonance in solution, but **5** cannot be isolated because it undergoes *σ-dimerization*, giving rise to a σ-bonded 1,1′-biphenalenyl (**6**) (Scheme 2).[9,10]

(1) Woodward, R. B.; Hoffmann, R. *J. Am. Chem. Soc.* **1965**, *87*, 2511.
(2) Gajewski, J. J. *Hydrocarbon Thermal Isomerizations*; Academic Press: New York, 1981; pp 166−76.
(3) (a) Ventura, E.; do Monte, S. A.; Dallos, M.; Lischka, H. *J. Phys. Chem. A* **2003**, *107*, 1175. (b) Staroverov, V. N.; Davidson, E. R. *J. Am. Chem. Soc.* **2000**, *122*, 186. (c) Sakai, S. *Int. J. Quantum Chem.* **2000**, *80*, 1099. (d) Kozlowski, P. M.; Dupius, M.; Davidson, E. R. *J. Am. Chem. Soc.* **1995**, *117*, 774. (e) Jiao, H.; Schleyer, P. v. R. *Angew. Chem., Int. Ed. Engl.* **1995**, *34*, 334. (f) Hrovat, D. A.; Morokuma, K.; Borden, W. T. *J. Am. Chem. Soc.* **1994**, *116*, 1072. (g) Wiest, O.; Black, K. A.; Houk, K. N. *J. Am. Chem. Soc.* **1994**, *116*, 10336. (h) Dewar, M. J. S.; Jie, C. *Acc. Chem. Res.* **1992**, *25*, 537.
(4) Reviews: (a) Staroverov, V. N.; Davidson, E. R. *J. Mol. Struct. (THEOCHEM)* **2001**, *573*, 81. (b) Wiest, O. In *Encyclopedia of Computational Chemistry*; Schleyer, P. v. R., Ed.; Wiley: Chichester, 1998; Vol. 5, p 3111 ff. (c) Borden, W. T.; Davidson, E. R. *Acc. Chem. Res.* **1996**, *29*, 67. (d) Houk, K. N.; Gonzalez, J.; Li, Y. *Acc. Chem. Res.* **1995**, *28*, 81.
(5) (a) Hrovat, D. A.; Chen, J.; Houk, K. N.; Borden, W. T. *J. Am. Chem. Soc.* **2000**, *122*, 7456. (b) Hrovat, D. A.; Beno, B. R.; Lange, H.; Yoo, H.-Y.; Houk, K. N.; Borden, W. T. *J. Am. Chem. Soc.* **1999**, *121*, 10529.
(6) Doering, W. v. E.; Wang, Y. *J. Am. Chem. Soc.* **1999**, *121*, 10112.
(7) Navarro-Vázquez, A.; Prall, M.; Schreiner, P. R. *Org. Lett.* **2004**, *6*, 2981.
(8) Hoffmann, R.; Woodward, R. B. *J. Am. Chem. Soc.* **1965**, *87*, 4389.

Scheme 2. σ-Dimerization of Phenalenyl Radical (**5**)

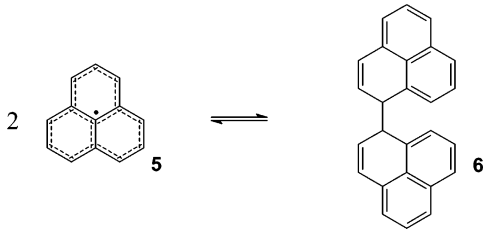

Scheme 3. π-Dimerization of 2,5,8-Tri-*tert*-butylphenalenyl Radical (**7**)

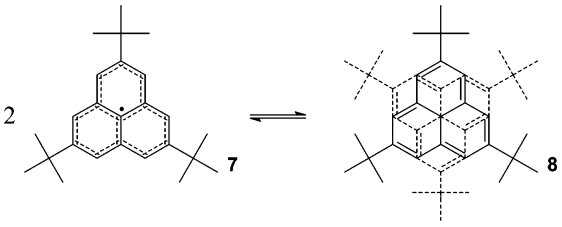

Recently there has been increasing interest in **5** and its derivatives, such as 2,5,8-tri-*tert*-butylphenalenyl radical,[11,12] perchlorophenalenyl radical,[13] and spiro-biphenalenyl radicals,[14−16] because of their diverse electrical, optical, and magnetic properties in the solid state. The solid-state structures of these radicals reveal the existence of another important packing motif of *π-dimerization*;[11,12,14,15] ESR and UV−vis also confirm π-dimerization in solution.[17] The π-dimerization of 2,5,8-tri-*tert*-butylphenalenyl radical (**7**) shown in Scheme 3 results from the pairing of the two π-electrons from the two SOMOs.[11,12,17] The intermolecular $\pi-\pi$ interaction associated with π-dimerization has been recently recognized as a new class of multicenter covalent π-bonding,[11b,12,17−19] bringing the two radicals slightly closer together (with an interplanar separation of 3.2−3.3 Å for **8**) than the sum of the van der Waals radii.[11] The binding energy for the staggered π-dimer **8** in CH_2Cl_2 solution is −9.5 and −8.8 kcal/mol according to ESR and UV−vis spectral measurements, respectively.[17] In comparison, the binding energy for the σ-dimer **6** is −11.3 kcal/mol in CCl_4 solution.[10,20,21] These π-dimers are paramagnetic,[11,14] while the σ-dimers exhibit diamagnetism.[10,14] Experimental and theoretical studies on different substituted phenalenyls indicate the energetic preference of σ-dimerization over π-dimerization by 1−5 kcal/mol.[21]

Scheme 4. Cope Rearrangement of Cyclo-biphenalenyl (**9**)

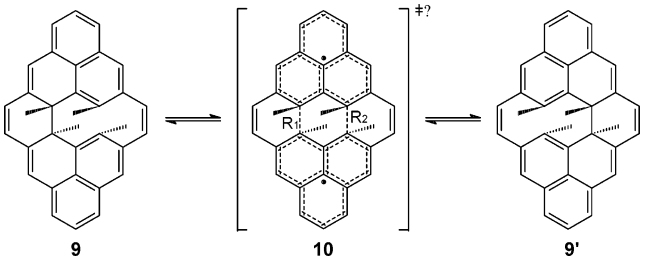

The analogy between the allyl radical and **5**, or that between their σ-dimers **1** and **6**, prompts one to propose the hypothetical Cope rearrangement of **6**; however, the study of such a Cope rearrangement is hindered by the presence of a dissociative path shown in Scheme 2.[9,10] X-ray diffraction shows that the title compound **9** (Scheme 4) has a σ-bond connecting the two phenalenyl units.[22,23] In contrast to **6**, the two etheno bridges in **9** maintain the proximity of the two phenalenyl units, thus making the Cope rearrangement possible. The Cope rearrangement of **9** (and its enantiomer **9′**) has been studied by dynamic NMR, showing an activation barrier of ∼9 kcal/mol.[23] Unlike the theoretically well-studied case of **1**, the Cope rearrangement of **9** has eluded the attention of theoretical investigators, and a number of questions remain unclear: What is the nature of the transition structure or possibly of the intermediate, **10**? What is the role of π-dimerization in the process? What is the length of the inter-phenalenyl distance R_1 (R_2) in **10**?[24] Can the structure of **10** be anticipated on the basis of the archetypal case of **1**?

Motivated by the increasing interest in **5** and its derivatives, and the availability of the experimental results on the Cope rearrangement of **9**, we explore herein the potential energy surface (PES) of **9**. We found that the Cope rearrangement of **9** is *stepwise*, proceeding through an unusual C_{2h} intermediate **10** with a relatively long inter-phenalenyl distance R ($R_1 = R_2 \approx 2.8$ Å), which is stabilized by multicenter covalent π-bonding as a result of π-dimerization during the Cope rearrangement process. To our best knowledge, this unusual intermediate with such a long inter-phenalenyl distance is the first example in the family of Cope rearrangements.

(9) (a) Reid, D. H. *Chem. Ind.* **1956**, 1504. (b) Gerson, F. *Helv. Chim. Acta* **1966**, *49*, 1463.
(10) Zheng, S.; Lan, J.; Khan, S. I.; Rubin, Y. *J. Am. Chem. Soc.* **2003**, *125*, 5786.
(11) (a) Goto, K.; et al. *J. Am. Chem. Soc.* **1999**, *121*, 1619. (b) Fukui, K.; Sato, K.; Shiomi, D.; Takui, T.; Itoh, K.; Gotoh, K.; Kubo, T.; Yamamoto, K.; Nakasuji, K.; Naito, A. *Synth. Met.* **1999**, *103*, 2257. (c) Suzuki, S.; Morita, Y.; Fukui, K.; Sato, K.; Shiomi, D.; Takui, T.; Nakasuji, K. *J. Am. Chem. Soc.* **2006**, *128*, 2530.
(12) Takano, Y.; Taniguchi, T.; Isobe, H.; Kubo, T.; Morita, Y.; Yamamoto, K.; Nakasuji, K.; Takui, T.; Yamaguchi, K. *J. Am. Chem. Soc.* **2002**, *124*, 11122.
(13) Koutentis, P. A.; Chen, Y.; Cao, Y.; Best, T. P.; Itkis, M. E.; Beer, L.; Oakley, R. T.; Cordes, A. W.; Brock, C. P.; Haddon, R. C. *J. Am. Chem. Soc.* **2001**, *123*, 3864.
(14) Liao, P.; Itkis, M. E.; Oakley, R. T.; Tham, F. S.; Haddon. R. C. *J. Am. Chem. Soc.* **2004**, *126*, 14297.
(15) Itkis, M. E.; Chi X.; Cordes, A. W.; Haddon R. C. *Science* **2002**, *296*, 1443.
(16) Pal, S. K.; Itkis, M. E.; Tham, F. S.; Reed, R. W.; Oakley, R. T.; Haddon, R. C. *Science* **2005**, *309*, 281.
(17) Small, D.; Zaitsev, V.; Jung, Y.; Rosokha, S. V.; Head-Gordon, M.; Kochi, J. K. *J. Am. Chem. Soc.* **2004**, *126*, 13850.
(18) Haddon, R. C. *Aust. J. Chem.* **1975**, *28*, 2343.
(19) Multicenter covalent π-bonding also occurs in charged π-radicals in addition to neutral ones. For $(TCNE)_2^{2-}$, see: (a) Lü, J. M.; Rosokha, S. V.; Kochi, J. K. *J. Am. Chem. Soc.* **2003**, *125*, 12161. (b) Novoa, J. J.; Lafuente, P.; Del Sesto R. E.; Miller, J. S. *Angew. Chem., Int. Ed.* **2001**, *40*, 2540. (c) Del Sesto, R. E.; Miller, J. S.; Lafuente, P.; Novoa, J. J. *Chem. Eur. J.* **2002**, *8*, 4894. (d) Jakowski, J.; Simons, J. *J. Am. Chem. Soc.* **2003**, *125*, 16089. (e) Jung, Y.; Head-Gordon, M. *Phys. Chem. Chem. Phys.* **2004**, *6*, 2008. For the oligothiophene π-dimer dication, see: (f) Brocks, G. *J. Chem. Phys.* **2000**, *112*, 5353.
(20) (a) The binding energy of **6** is slightly smaller in toluene solution (−9.8 ± 0.7 kcal/mol), because of the increase in solvation strength through $\pi-\pi$ interactions of **5** with this solvent,[10] which favors the dissociation of **6**. (b) We choose to use the binding energy of **6** measured in CCl_4 solution to compare with that of **8** measured in CH_2Cl_2 because of the similarity of solvents.
(21) Recent ESR spectral measurements of **6** provided a similar binding energy of −10 ± 1 kcal/mol in CH_2Cl_2 solution. See: (a) Small, D.; Rosokha, S. V.; Kochi, J. K.; Head-Gordon, M. *J. Phys. Chem. A* **2005**, *109*, 11261. (b) Zaitsev, V.; Rosokha, S. V.; Head-Gordon, M.; Kochi, J. K. *J. Org. Chem.* **2006**, *71*, 520.
(22) Systematic nomenclature is dehydro-*anti*-4,5,15,16-tetramethyl[2$_2$](5,8)-phenalenophane-1,12-diene. We call it cyclo-biphenalenyl for convenience, where "cyclo" is used to denote the cyclophane structure rendered by the two etheno bridges.
(23) Rohrbach, W. D.; Boekelheide, V.; Hanson, A. W. *Tetrahedron Lett.* **1985**, *26*, 815.
(24) The inter-phenalenyl distance of **10** is analogous to the inter-allylic bond lengths of **2**, **3**, and **4**. The same term is used for **13**, and for **14** this becomes the inter-naphthalene distance.

Table 1. Experimental Geometries of **9** and Calculated Geometries for the Global Minimum of **9**, the Cope Transition Structure, and the Two Intermediates Found with R(U)B3LYP/6-31G*[a]

	X-ray structure	global minimum of **9**		transition structure	π-intermediate **10** ($R_1 = R_2$)		aromatic intermediate **11** ($R_1 = R_2$)	
index	of **9**[b]	RB3LYP[c]	RB3LYP[d]	RB3LYP[c,e]	RB3LYP	UB3LYP	RB3LYP	UB3LYP
symmetry	C_2	C_2	C_2	C_2	C_{2h}	C_{2h}	C_{2h}	C_{2h}
C1−C2	1.32	1.354	1.347	1.351	1.351	1.352	1.391	1.368
C2−C3	1.47	1.460	1.456	1.473	1.482	1.485	1.420	1.447
C3−C4	1.56, 1.51[f]	1.529	1.526	1.474	1.437	1.427	1.530	1.524
C4−C4′	1.61, 1.62[f]	1.561	1.556	1.529	1.514	1.513	1.584	1.575
C4−C10c	1.48, 1.50[f]	1.535	1.533	1.469	1.441	1.442	1.529	1.521
C3−C11	1.36	1.352	1.345	1.361	1.378	1.387	1.381	1.362
C10a−C11	1.43	1.446	1.442	1.437	1.422	1.417	1.415	1.437
C10a−C10b	1.42	1.434	1.430	1.431	1.430	1.430	1.476	1.452
C10b−C10c	1.44	1.438	1.434	1.447	1.448	1.445	1.361	1.392
C10−C10a	1.39	1.390	1.386	1.398	1.410	1.414	1.399	1.398
C9−C10	1.38	1.407	1.403	1.400	1.391	1.392	1.397	1.398
C8−C9	1.36	1.379	1.373	1.384				
C7a−C8	1.38	1.419	1.415	1.414				
C7a−C10b	1.43	1.431	1.426	1.429				
C7−C7a	1.42	1.418	1.413	1.421				
C6−C7	1.36	1.378	1.372	1.376				
C5−C6	1.48, 1.43[f]	1.444	1.440	1.443				
C5−C10c	1.43, 1.46[f]	1.406	1.401	1.422				
C5−C5′	1.45, 1.47[f]	1.519	1.514	1.517				
C6−C12	1.47	1.484	1.481	1.482				
C12−C13	1.32	1.355	1.348	1.353				
C4−C16 (R_1)	1.63	1.684	1.685	2.236	2.820	3.030	1.554	1.587
C5−C15 (R_2)	2.65	2.686	2.694	2.714				

[a] Atomic numbering for all structures follows **9** shown in Chart 1. The characteristics of the intermediates are discussed in the text. [b] Bond lengths from X-ray measurements, taken from Figure 1 in ref 23. [c] RB3LYP result is the same as that of UB3LYP. [d] Geometry is also optimized with a larger basis set of 6-311+G(2d) to check the basis set effect. [e] Only one transition structure is found, connecting the global minimum **9** and the π-intermediates **10** found by R(U)B3LYP. [f] The bonds involving C4 and C5 atoms have two values each because atoms C4 and C5 were each modeled as two centers as a result of four-fold disorder described in ref 23.

Computational Methodology

The PES of **9** was explored by geometry optimization, by a relaxed PES scan along the C_{2h} symmetry cut ($R_1 = R_2 = R$), and by transition state searches. Calculations were performed at the level of DFT using Becke's three-parameter hybrid functional in combination with Lee−Yang−Parr correlation functional (B3LYP)[25] and the 6-31G* basis set.[26] This level of theory has been applied to the Cope rearrangements of unsubstituted and substituted **1**, giving good agreements with experiments.[3g,5] Both the spin-restricted method (RB3LYP) and the broken-symmetry, spin-unrestricted method (UB3LYP) were employed. Vibrational analysis was performed at each stationary point to verify its identity as a minimum or a transition state. Triplet energies used for magnetic susceptibility calculations are obtained from single-point calculations using the singlet geometries found by the optimizations.

Staroverov and Davidson suggested that the BPW91 functional instead of hybrid DFT should be used to avoid spurious stationary points when studying sigmatropic rearrangements.[27,28] To rule out this concern, we also performed a relaxed PES scan for **9** with R(U)BPW91 along the C_{2h} symmetry cut with the 6-31G* basis set.

^{1}H NMR chemical shielding tensors were evaluated using the GIAO method[29] at the B3LYP /6-31G* level of theory for the global minimum and the Cope intermediate of **9** found with RB3LYP/6-31G*. ^{13}C NMR chemical shielding tensors and nucleus-independent chemical shifts (NICS)[30] were evaluated similarly and are discussed in the NMR section. The calculated chemical shielding constants were referenced to those of tetramethylsilane (TMS, 32.1821 ppm for ^{1}H and 189.7710 ppm for ^{13}C) calculated by the same methodology.

Chart 1. Atomic Numbering[23] of Cyclo-biphenalenyl **9**

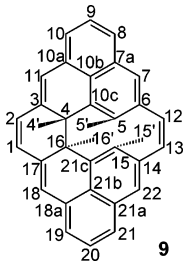

9

Results and Discussion

Potential Energy Surface. First, the global minimum on the PES of **9** was identified with $R_1 \neq R_2$ using RB3LYP/6-31G* optimization. UB3LYP optimization gives the same geometry. This C_2 structure corresponds to the degenerate σ-bonded Cope reactant or product (**9** or **9′**, see Scheme 4). Its geometry is compared with the X-ray structure in Table 1. More than half of the bond lengths agree well with the X-ray data; the largest discrepancy stands out for bonds involving atoms C4 and C5, e.g., C4−C4′ and C5−C5′. The experimental 1.61 or 1.62 Å for C4−C4′ is probably a little too long for a bond between two sp^3-hybridized carbon atoms, and the experimental 1.45 or 1.47 Å for C5−C5′ is obviously a little too short for a bond between sp^2- and sp^3-hybridized carbon atoms.[31] This discrepancy may come from the four-fold disorder of the crystal

(25) (a) Becke, A. D. *J. Chem. Phys.* **1993**, *98*, 5648. (b) Lee, C.; Yang, W.; Parr, R. G. *Phys. Rev. B* **1988**, *37*, 785.
(26) All calculations are performed with GAUSSIAN98: Pople, J. A.; et al. *Gaussian 98*, revision A. 11.4; Gaussian, Inc.: Pittsburgh, PA, 2002.
(27) Staroverov, V. N.; Davidson, E. R. *J. Am. Chem. Soc.* **2000**, *122*, 7377.
(28) For the Perdew−Wang correlation functional, see: Perdew, J. P.; Wang, Y. *Phys. Rev. B* **1992**, *45*, 13244.
(29) Wolinski, K.; Hinton, J. F.; Pulay, P. *J. Am. Chem. Soc.* **1990**, *112*, 8251.
(30) Chen, Z.; Wannere, C. S.; Corminboeuf, C.; Puchta, R.; Schleyer, P. v. R. *Chem. Rev.* **2005**, *105*, 3842.
(31) Pople, J. A.; Gordon, M. *J. Am. Chem. Soc.* **1967**, *89*, 4253

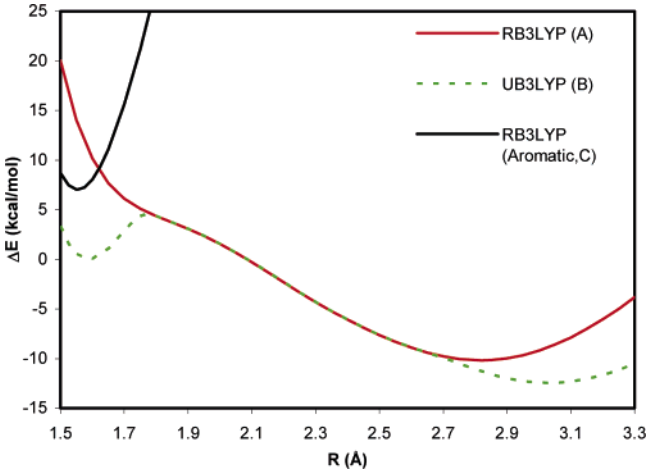

Figure 1. C_{2h} symmetry cuts ($R_1 = R_2 = R$) through the PES at the levels of R(U)B3LYP/6-31G* for the Cope rearrangement of **9**.

structure, as noted by the authors themselves, stating that the X-ray data may not correctly represent individual bond lengths.[23] This problem also manifests in the values of R_1 and R_2, which also involve C4 and C5, as shown by the optimized $R_1 = 1.684$ Å and $R_2 = 2.686$ Å values compared with the respective X-ray diffraction values of 1.63 and 2.65 Å. The R_1 bond length is elongated, which is also observed in a σ-bonded spiro-biphenalenyl dimer.[14] Optimization with a larger basis set at 6-311+G(2d) gives virtually the same geometry as that obtained with 6-31G*. NMR data also support this structure as the global minimum because the calculated chemical shifts agree well with the experiment (see the NMR section).

Essential information about the mechanism of Cope rearrangements can be obtained by studying a C_{2h} symmetry cut through the PES.[27] The relaxed PES scans for **9** along the C_{2h} cut are shown in Figure 1. In contrast to the Cope rearrangement of **1**, we did not find a saddle point of C_{2h} symmetry from $R =$ 1.7 to 2.6 Å. Instead, we found two minima along the C_{2h} cut outside the said range: one at the small-R end and the other at the large-R end. With RB3LYP (curve A in Figure 1), we found only one minimum at $R = 2.820$ Å. With UB3LYP (curve B), the solutions are different from those obtained with RB3LYP at both the small-R end and the large-R end. For $R \leq 1.78$ Å, the UB3LYP curve (B) departs from curve A, and there is an additional minimum at $R = 1.587$ Å. For $R \geq 2.65$ Å, curve B also departs from curve A, and the corresponding minimum shifts some from $R = 2.820$ to 3.030 Å. The geometries of those intermediates are given in Table 1. In the following, we discuss the characteristics of these minima.

First, we address the nature of the minimum at the small-R end found by UB3LYP and why RB3LYP and UB3LYP behave differently around that minimum (curves A and B in Figure 1). It turns out that, in addition to inter-phenalenyl distance R, there exists another important degree of freedom, which is the bond length alternation ($\delta = R_{C=C} - R_{C-C}$) on the etheno bridges.[32] We found another RB3LYP solution with smaller δ, which is shown in Figure 1 as curve C with a minimum at $R = 1.554$ Å. The structure of this minimum is characteristic of its small δ values (this can be calculated from the data in Table 1) and the near-planarity of the annulene-like periphery. The region of

Chart 2. Comparison of the Aromatic Intermediate **11** and Aromatic Dimethyldihydropyrene **12**[a]

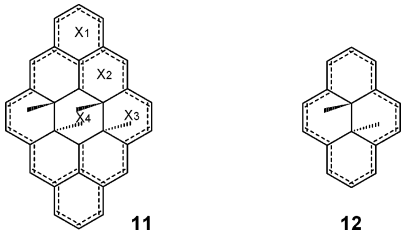

11 **12**

[a] Dummy atoms X_1-X_4 at the six-membered ring centers are used to define the locations for NICS calculations; see the NMR section.

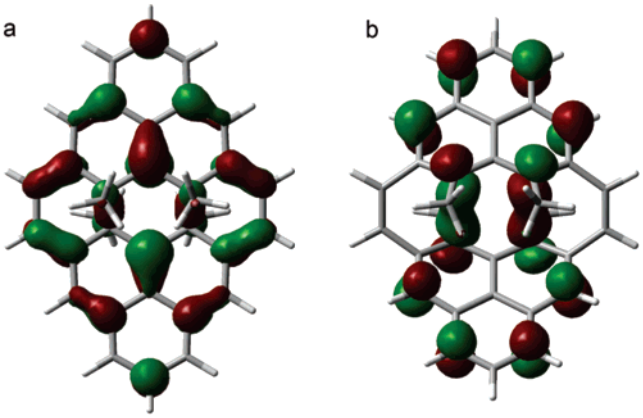

Figure 2. HOMOs of the aromatic intermediate **11** (a) and the π-intermediate **10** (b) calculated using RB3LYP/6-31G*. For the π-intermediate, note the absence of significant wavefuntion contributions from the etheno bridges. Side views of these HOMOs, showing the planarity of **11** and the π-dimer character of **10**, are given in the Supporting Information.

small alternation extends to the adjacent rings connected to the bridges. Its geometry can be described by two σ-bonds connecting the phenalenyl units, with the rest of the π-electrons forming an aromatic system ($26\pi+2\times2\sigma$). This *aromatic intermediate* **11** has a fully delocalized structure, corresponding to its C_{2h} symmetry. **11** is analogous to the experimentally well-characterized "model" aromatic molecule dimethyldihydropyrene **12** (Chart 2),[33] which also has a small δ value on its remarkably planar periphery.[34] The internal methyl protons of **12** have been used as a probe for aromaticity.[30,35] NMR calculations are compared for the internal methyl protons between **11** and **12** to support the aromaticity of **11** (see the NMR section). As can be seen from Figure 2a, the highest occupied molecular orbital (HOMO) of this aromatic intermediate does not have any phenalenyl SOMO character but involves contributions from the etheno bridges. Due to the aromatic character of this minimum at $R = 1.554$ Å, curve C is termed the aromatic curve. On the other hand, curve A represents the structures with larger δ and less planarity. Beyond the crossover point of curves A and C at $R \approx 1.63$ Å, the two σ-bonds become less stable, and the structures on curve A resemble π-dimers.

(32) (a) Kertesz, M.; Choi, C. H.; Yang, S. *Chem. Rev.* **2005**, *105*, 3448. (b) Choi, C. H.; Kertesz, M. *J. Chem. Phys.* **1998**, *108*, 6681.

(33) (a) Boekelheide, V.; Phillips, J. B. *Proc. Natl. Acad. Sci. U.S.A.* **1964**, *51*, 550. (b) Boekelheide, V.; Phillips, J. B. *J. Am. Chem. Soc.* **1967**, *89*, 1695. (c) Hopf, H. *Angew. Chem., Int. Ed.* **2003**, *42*, 5540.

(34) (a) Williams, R. V.; Edwards, W. D.; Vij, A.; Tolbert, R. W. *J. Org. Chem.* **1998**, *63*, 3125. (b) Mitchell, R. H.; Iyer, V. S.; Khalifa, N.; Mahadevan, R.; Venugopalan, S.; Weerawarna, S. A.; Zhou, P. *J. Am. Chem. Soc.* **1995**, *117*, 1514.

(35) (a) Mitchell, R. H. *Chem. Rev.* **2001**, *101*, 1301. (b) Williams, R. V.; Armantrout, J. R.; Twamley, B.; Mitchell, R. H.; Ward, T. R.; Bandyopadhyay, S. *J. Am. Chem. Soc.* **2002**, *124*, 13495.

Chart 3. Dehydro-*anti*-4,5,15,16-tetramethyl[2_2](5,8)phenalenophane

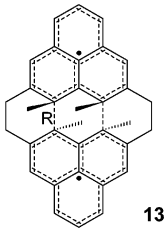

13

The longest R value that can exist on curve C is 1.9 Å, beyond which point the aromatic curve C reduces to curve A and the four σ-electrons are reallocated to π-conjugation. This value is consistent with the longest C−C bond length known experimentally and theoretically.[36] The structures on curves B and C near 1.6 Å are similar to each other with respect to alternation and planarity. Thus, we conclude that the UB3LYP minimum at $R = 1.587$ Å is also an aromatic intermediate, similar to the RB3LYP solution with $R = 1.554$ Å. The UB3LYP solution has lower energy than the RB3LYP solution for this aromatic intermediate, as can be seen from Figure 1. The energies of the aromatic intermediate approximated by these two similar structures on curves B and C are too high, and therefore the aromatic intermediate does not play a role in the Cope rearrangement of **9**.

Further support for the aromatic character of the above-mentioned aromatic intermediate at the short-R end comes from a comparison with **13** (Chart 3), where two saturated ethano bridges replace the two etheno bridges in **9** or **10**. Figure 3 shows the C_{2h} cuts through the PES of **13**. In contrast to the PES of **9** shown in Figure 1, there is a minimum at $R = 2.905$ Å (RB3LYP) and 3.261 Å (UB3LYP), but there is no minimum at the small-R end, because the aromatic conjugation along the periphery is disrupted for **13**.

Next we turn to the minimum at $R = 2.820$ Å (RB3LYP) or 3.030 Å (UB3LYP) in Figure 1. As can be seen from Figure 2b, the HOMO of the RB3LYP minimum has no significant contribution from the etheno bridges but mostly involves two phenalenyl SOMOs interacting through space via a four-center $\pi-\pi$ overlap. Therefore, the RB3LYP minimum has π-dimer character and can be described as a $2\times13\pi+2\times2\pi$ system, where 13π denotes the phenalenyl unit and 2π denotes the etheno bridge unit. The UB3LYP minimum has the same π-dimer character as the RB3LYP solution but has lower energy. The energy of the UB3LYP minimum is even lower (see the energetics section) than that of the σ-bonded reactant **9**, which is the global minimum, and so the UB3LYP optimization produces in this case an artifact. (We will see in the following that RBPW91 and UBPW91 do not have this problem and these two methods provide the same solution.) We conclude that the minimum at the long-R end is best described by the RB3LYP solution at $R = 2.820$ Å. This inter-phenalenyl distance R is comparable to the shortest intradimer C−C distance (2.83 Å) experimentally found for a tetracyanoethylene (TCNE) dimer

(36) (a) Komarov, I. V. *Russ. Chem. Rev.* **2001**, *70*, 991. (b) Toda, F.; Tanaka, K.; Stein, Z.; Goldberg, I. *Acta Crystallogr., Sect. C* **1996**, *52*, 177. (c) Kaupp, G.; Boy, J. *Angew. Chem., Int. Ed. Engl.* **1997**, *36*, 48. (d) Choi, C. H.; Kertesz, M. *Chem. Commun.* **1997**, 2199. (e) Brown, D. A.; Clegg, W.; Colquhoun, H. M.; Daniels, J. A.; Stephenson, I. R.; Wade, K. *Chem. Commun.* **1987**, 889. (f) Isea, R. *J. Mol. Struct. (THEOCHEM)* **2001**, *540*, 131.

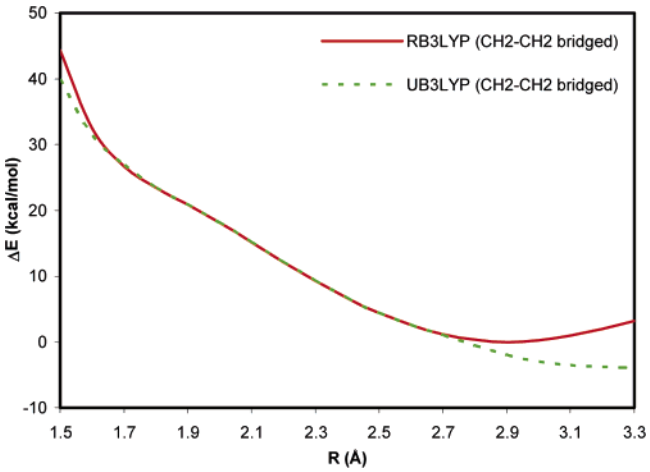

Figure 3. C_{2h} cuts through the PES at the levels of R(U)B3LYP/6-31G* for **13**.

dianion[19b] and is shorter than the van der Waals value, displaying a through-space covalent π-bonding interaction between the two phenalenyl units. Weak covalent π-bonding between π-conjugated neutral and charged radicals has been recognized recently as a novel and important bonding interaction.[12,17,19] The key point is that the π-bonding interaction associated with π-dimerization stabilizes this π-bonded structure with relatively long CC contacts, similar to other π-dimers.[12,14,15,19] Now we can answer the questions raised at the beginning regarding the Cope rearrangement of **9** depicted in Scheme 4. The Cope rearrangement of **9** proceeds through a *π-intermediate* **10**, because it has much lower energy than the aromatic intermediate **11**.

To complete the PES of **9**, we identified the transition structure connecting the C_2 reactant and the C_{2h} π-intermediates (both RB3LYP and UB3LYP geometries). (Since the aromatic intermediate **11** does not play a role in the Cope rearrangement of **9**, we did not calculate the reaction path through it.) The obtained transition structure is given in Table 1. Regardless of the theoretical levels used, we obtained only one C_2 transition structure at $R_1 = 2.263$ Å and $R_2 = 2.714$ Å. As can be seen from the schematic diagram of the PES in Figure 4, the reaction path with RB3LYP is different from that with UB3LYP only near the π-intermediate. Normal-mode analysis of the only imaginary frequency of the transition structure corresponds to σ-bond-breaking. On the basis of energetics shown in the next section, we believe that the actual reaction follows more closely the RB3LYP path. This reaction path can be described as a stepwise rearrangement where σ-bond-breaking and multicenter π-bonding take place simultaneously.

The stepwise Cope rearrangement mechanism of **9** is completely different from the archetypal Cope rearrangement of **1**, and the intermediate structure **10** cannot be anticipated on the basis of the knowledge of the Cope rearrangement of **1**. On the basis of a comprehensive study on a large set of Cope-like reactions, Schreiner and co-workers derived a simple rule for the Cope reaction family, stating that a stepwise reaction takes place when the intermediates are stabilized by either allyl or aromatic resonance.[7] All of the intermediates studied therein involve inter-allyl distances around 1.6 Å. In contrast to those previously studied Cope rearrangements,[5,7] the current Cope intermediate **10**, with such a long inter-phenalenyl distances $R = 2.820$ Å, is unparalleled. Our finding is thus an extension to

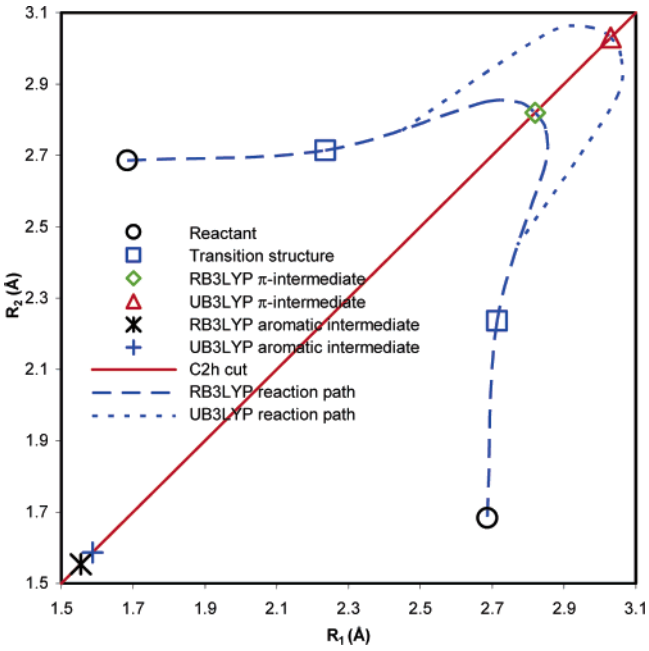

Figure 4. Schematic diagram of the PES of **9** as a function of R_1 and R_2. The coordinates of all stationary points come from calculations (see Table 1). The red diagonal line is the C_{2h} cut through the PES discussed in the text. The corresponding potential energy curves along the C_{2h} cut are given in Figure 1.

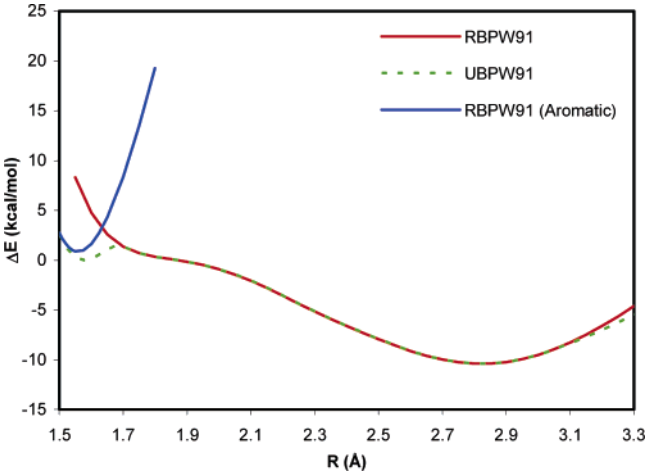

Figure 5. C_{2h} cuts through the PES at the levels of R(U)PW91 with 6-31G* basis set for Cope rearrangement of **9**. The total energy difference (ΔE) is relative to the minimum energy at $R = 1.578$ Å found with UPW91.

the Schreiner rule, in that the intermediate is stabilized by a through-space multicenter covalent π-bonding interaction.

We also performed a relaxed PES scan with R(U)BPW91 along the C_{2h} cut of **9** in order to avoid any bias related to the form of the density functionals.[27] We obtained conclusions similar to those found with the hybrid B3LYP functional. As can be seen in Figure 5, there are two minima at $R \approx 1.6$ and 2.8 Å. The only difference from the hybrid B3LYP results is that the UBPW91 curve departs from the RBPW91 curve at a much larger R value of 3.05 Å; therefore, UBPW91 produces the same minimum as RBPW91 at the large-R end. This shows the dependence of the π-intermediate's geometry on the theory used. The DFT calculations on the π-dimer of **5** by Takano et al.[12] have shown that broken-symmetry results are quite common for $\pi-\pi$ interacting biphenalenyls with UB3LYP. With a decreased amount of exchange in the DFT used, it is less likely to obtain broken-symmetry results, which explains why the UBPW91 does not give a different stationary point at the large-R end.

Energetics. The energies of some important stationary points on the PES of **9** are summarized in Table 2, together with those of **13**. The aromatic intermediates of **9** are high in energy and therefore do not contribute to the Cope rearrangement of **9**; those data are not discussed here but are available in the Supporting Information.

The RB3LYP energy for the π-intermediate **10** is higher than that of the σ-bonded reactant **9** by 3.4 kcal/mol, and by 1.7 kcal/mol with the zero-point energy correction (ZPE), consistent with the experimental energy differences between σ- and π-dimers of various unsubstituted and substituted phenalenyls.[10,17,21] This RB3LYP solution also agrees with the fact that the X-ray diffraction found the σ-bonded **9** instead of the π-intermediate **10**. The activation barrier from the reactant to the intermediate was calculated to be 6.3, 5.1, and 4.6 kcal/mol in terms of total energy, enthalpy, and Gibbs free energy (at room temperature 298 K, RT), respectively. Using a larger basis set of 6-311+G(2d), we optimized both **9** and **10**, from which the transition structure is obtained also with this larger basis set, giving the Cope rearrangement barrier of 5.7 kcal/mol in terms of total energy, compared to the value of 6.3 kcal/mol found with 6-31G* basis set. These barrier energies are lower than the 9 ± 1 kcal/mol value obtained from the dynamic NMR experiment.[23] Prior to the theoretical study presented herein, Rohrbach et al.[23] presumably used the formula for a concerted two-site and equal population reaction process to analyze the experimental NMR data. For a stepwise process, the rate constant from the reactant to the intermediate is twice as large as the apparent rate constant for the reaction observed by dynamic NMR, and so the value of the activation barrier is slightly different compared to that for the concerted process.[37] From the theoretical side, B3LYP/6-31G* has proved to be very successful for the energetics of the Cope rearrangement of unsubstituted and substituted **1**.[3g,5] However, the spin contamination, as shown by the expectation value of the total spin angular momentum of $\langle S^2 \rangle = 0.50$ of the UB3LYP-optimized **10**, indicates that a higher level of theory (e.g., CASSCF, albeit impractical for such large systems) would provide more accurate estimates for the π-intermediate with an open-shell singlet character. Further experimental and theoretical investigations are necessary to reconcile the discrepancy between the experimental and the theoretical reaction barriers. Nevertheless, the calculated barrier is consistent with a stepwise rearrangement where σ-bond-breaking and multicenter π-bonding take place simultaneously.

In contrast to **9**, the π-bonded C_{2h} "intermediate" of **13** has a lower energy than that of the σ-bonded C_2 "reactant" by 2.6 kcal/mol based on RB3LYP optimization; therefore, the π-bonded structure is the global minimum, and Cope rearrangement is not possible for **13**. The UB3LYP optimization gives an $\langle S^2 \rangle$ value of 0.54, indicating an open-shell singlet character, similar to **10**. The UB3LYP energy is lower than the RB3LYP energy; however, according to what we understand for the π-bonded intermediate of **9**, we conclude the RB3LYP-optimized geom-

(37) Friebolin, H. *Basic One- and Two-Dimensional NMR spectroscopy*; Wiley-VCH Verlag GmbH: Weinheim, Germany, 1998; pp 311−312.

Table 2. Total Energies, Zero-Point Energies, and Total Spin Expectation Values of Some Stationary Points on the PES of **9** and **13**

	stationary points	theories	total energies (hartree)	ZPE (hartree)	$\langle S^2 \rangle$
9	global minimum	R(U)B3LYP	−1311.2224	0.4957	0.00
	transition structure	R(U)B3LYP	−1311.2123	0.4936	0.00
	π-intermediate **10**	RB3LYP (singlet)	−1311.2171	0.4930	0.00
		UB3LYP (triplet)[a]	−1311.2048		2.01
		UB3LYP (singlet)	−1311.2207	0.4916	0.50
13	σ-bonded structure	R(U)B3LYP	−1313.6641	0.5454	0.00
	π-bonded structure[b]	RB3LYP (singlet)	−1313.6682	0.5418	0.00
		UB3LYP (triplet)[a]	−1313.6614		2.01
		UB3LYP (singlet)	−1313.6744	0.5398	0.67

[a] Calculated using the RB3LYP singlet geometry; used for paramagnetism calculations shown in Figure 9. [b] Secondary saddle point; see text for discussion.

Chart 4. *anti*-4,5,14,15-Tetramethyl[2_2](2,7)naphthalenophane-1,11-diene

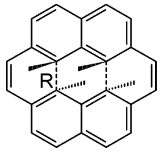

14

Table 3. Inter-naphthalene Distance *R* of Neutral, Dication, and Dianion of **14** Compared with the Inter-phenalenyl Distance *R* of **10**

	theory	symmetry	*R* (Å)[a]
10	RB3LYP [b]	C_{2h}	2.820
14	R(U)B3LYP	C_{2h}	3.207
$\mathbf{14}^{2+}$	R(U)B3LYP	C_{2h}	2.883
$\mathbf{14}^{2-}$	R(U)B3LYP	C_{2h}[c]	2.976
	R(U)B3LYP	C_2[d]	2.989 (R_1)
			3.008 (R_2)

[a] In case of C_2 symmetry, there are two *R* values, i.e., R_1 and R_2. [b] The UB3LYP solution is an artifact (see discussion in the PES section). [c] Second-order saddle point. [d] This distorts slightly from the C_{2h} structure. The other C_2 structure, with R_1 and R_2 exchanged, is equivalent. The C_{2h} second-order saddle point is flanked by these two C_2 minima. With ZPE included, the C_{2h} saddle point has lower energy than these two C_2 minima.

etry is more reliable. Vibrational calculations indicate that this RB3LYP geometry is a second-order saddle point, and yet normal-mode analysis reveals that the two imaginary frequency modes are floppy rotational modes of methyls. Thus, we conclude that this π-bonded C_{2h} structure is very close to the global minimum of **13** in terms of energy and geometry (see also the discussion on $\mathbf{14}^{2-}$). The synthesis of **13** should lead to the π-bonded structure, similar to the π-intermediate in the Cope rearrangement of **9**.

Covalent π-Bonding Effect. Further evidence for the stabilizing effects of π-bonding in the π-intermediate **10** can be obtained by investigating cyclophane **14**, which consists of two naphthalene units linked together by two etheno bridges (Chart 4). In contrast to **10**, where each phenalenyl unit has one unpaired π-electron, the etheno-bridged naphthalene units of **14** are closed-shell fragments. The inter-naphthalene distance *R* of **14** and those of the dication and dianion of **14** are compared in Table 3, together with the inter-phenalenyl distance of **10**. For neutral and charged **14**, UB3LYP provides the same structure as RB3LYP, unlike **10**, where the UB3LYP result is slightly different from the RB3LYP result (Tables 1 and 3). As expected, neutral **14** has a relatively longer *R* value of 3.2 Å compared to **10**, showing the absence of a covalent π-bonding effect for **14**.

Addition of two electrons to the lowest unoccupied molecular orbital (LUMO) of **14** provides an electron pair, leading to a significant reduction of *R* from 3.207 to 2.976 Å. Similar to the well-studied four-center, two-electron π-bonding of the TCNE π-dimer dianion,[19b−d] the π-bonding effect in $\mathbf{14}^{2-}$ comes from the interacting naphthalene LUMOs. Removal of two electrons from the HOMO of **14** gives $\mathbf{14}^{2+}$, with the inter-naphthalene distance also reduced significantly to 2.883 Å, due to covalent π-bonding effect coming from the interacting naphthalene HOMOs, similar to the oligothiophene π-dimer dication.[19e] The structures of $\mathbf{14}^{2+}$ and $\mathbf{14}^{2-}$ (also **13**) have π-dimer characteristics, similar to the π-intermediate **10** depicted in Figure 2b and Figure 1Sb. The inter-naphthalene distances *R* in the $\mathbf{14}^{2+}$ and $\mathbf{14}^{2-}$ cases are slightly longer than the inter-phenalenyl distance *R* of **10** (Table 3). This may be ascribed to the Coulombic repulsion that should work against such shortening of *R* in $\mathbf{14}^{2+}$ and $\mathbf{14}^{2-}$. We found that the C_{2h} structure of $\mathbf{14}^{2-}$ is a second-order saddle point. The two imaginary frequencies correspond to the rotations of methyls, exactly as in **13**. Here we went further to search for the minimum and found two such distorted C_2 structures flanking the C_{2h} saddle point. The geometries of the two C_2 structures are very close to that of the saddle point. Although the energies of these distorted C_2 structures are lower than the C_{2h} saddle point by ∼0.6 kcal/mol, with ZPE correction included, their energies become slightly higher than the C_{2h} saddle point, which comes about as a result of the two imaginary frequencies.

The above-mentioned $\mathbf{14}^{2-}$ is also optimized at the R(U)-B3LYP level, with only one of the two *R* values reduced significantly to 1.759 Å (the other becomes 2.726 Å), which gives an optimized geometry for the σ-bonded structure similar to **9**. The total energy of the optimized σ-bonded C_2 structure is higher than that of the π-bonded structure of $\mathbf{14}^{2-}$ by 10.6 kcal/mol; therefore, similar to **13**, Cope rearrangement is not possible for $\mathbf{14}^{2-}$, either. Thus, we conclude that the global minimum of $\mathbf{14}^{2-}$ should be the doubly degenerate π-bonded C_2 structure (see footnote *d* in Table 3), and the vibrationally averaged structure is the π-bonded C_{2h} structure. This structure can be confirmed by comparing our calculated NMR spectra with the experimental NMR spectra.

NMR Spectroscopy. We compare the calculated NMR chemical shifts with the available experiments in order to lend further experimental support to the structures discussed in this paper. As can be seen from Figure 6, the experimental ^{1}H NMR spectrum of **9** at RT[23] shows one chemical shift at 1.5 ppm for the 12 protons from the four methyls. Theoretical NMR calculations for the σ-bonded **9** provide six different chemical

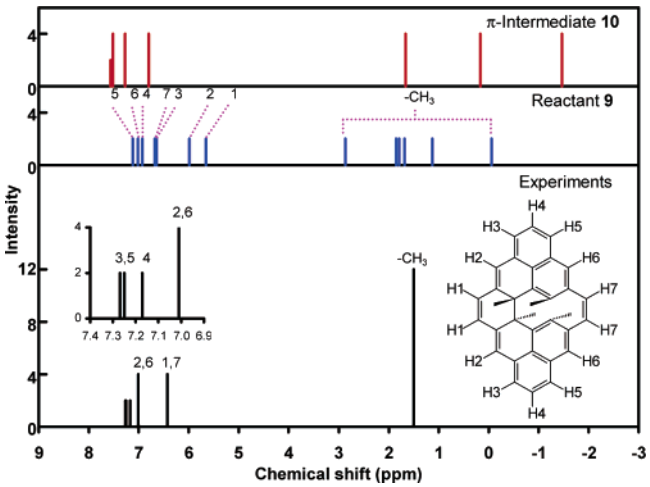

Figure 6. Experimental ^{1}H NMR spectrum of **9** at RT from ref 23, compared with calculated peaks from B3LYP/6-31G*. Chemical shift is relative to TMS.

shifts for methyls (two protons each). This discrepancy can be explained by the fact that floppy methyls undergo rotation, and therefore fast exchange of the protons leads to coalescence of the six groups of proton signals into two peaks, and the Cope rearrangement will lead to a further coalescence into one peak. The other calculated proton chemical shifts for the σ-bonded **9** can be explained similarly: H1 and H7 coalesce, and H2 and H6 coalesce, while H4 stays the same (a multiplet). H3 and H5 also coalesce, but experimental NMR shows two peaks at 7.25 and 7.27 ppm, and these were interpreted, probably incorrectly, as singlets.[23] As a matter of fact, H3 and H5 should exhibit doublet signals. Therefore, the peaks at 7.25 and 7.27 ppm are due to the coalesced H3 and H5 doublets. In comparison, the calculated chemical shifts for the π-intermediate **10** agree less well with the experimental NMR spectrum. The energy difference of 1.7 kcal/mol (with ZPE correction) gives a Boltzmann occupancy ratio of 0.031 between the π-intermediate and the degenerate reactant and product at RT, explaining the fact that the X-ray diffraction found only the structures of the σ-bonded **9** and **9′**. With such a small ratio, it is very unlikely that the π-intermediate would be observed by NMR spectroscopy, either. It can thus be concluded that the NMR belongs to the σ-bonded **9**. To investigate the basis set effects on the NMR spectrum, we also performed calculations for **9** and **10** with a larger basis set of 6-311+G(2d), using the B3LYP/6-311+G(2d)-optimized geometries. These calculations provide similar results (the comparison with experimental NMR is provided in the Supporting Information), indicating that the basis set of 6-31G* is sufficient for the current work; therefore, for the rest of the NMR calculations, we stick to the 6-31G* basis set.

^{1}H NMR chemical shifts are also calculated for the aromatic intermediate **11** found by both RB3LYP and UB3LYP. Experimentally, NMR spectroscopy is the most frequently used technique, providing criterion for characterizing aromaticity.[30,35,38] The internal methyl protons of **12** are shifted upfield (shielded) with a chemical shift of −4.25 ppm, indicating aromaticity of the 14π-electron periphery of **12**.[30,35] Our calculated chemical shifts of the internal methyl protons for the aromatic intermediate **11** found by RB3LYP are −5.40, −5.51, and −5.72 ppm. Fast exchange due to methyl rotation should lead to coalescence of these three signals to one peak located somewhere between −5.4 and −5.7 ppm. These methyl protons are shifted upfield relative to those of the π-intermediate and the global minimum of **9** (see Figure 6). For the aromatic intermediate geometry found by UB3LYP, the calculated chemical shifts of the internal methyl protons are −4.24, −4.40, and −4.96 ppm. The methyl protons of the RB3LYP geometry are shifted more upfield than those of the UB3LYP geometry by ca. 1 ppm, indicating that the RB3LYP geometry has a higher degree of aromaticity. This trend agrees with the smaller bond length alternation for the RB3LYP geometry described earlier. Meanwhile, the UB3LYP geometry has a relatively long *R* value of 1.587 Å for an C(sp^3)−C(sp^3) bond,[31] and therefore the RB3LYP geometry is probably more reliable.

Table 4. NICS Values (ppm) for the Aromatic Intermediate **11**

dummy atoms[a]	RB3LYP geometry		UB3LYP geometry	
	1 Å above[b]	1 Å below[b]	1 Å above[b]	1 Å below[b]
X_1	−20.3	−23.0	−18.3	−20.9
X_2	−11.8	−16.5	−10.2	−14.6
X_3	−17.1	−17.2	−16.0	−16.0
X_4	−10.8	−10.8	−8.1	−8.1

[a] Locations defined in Chart 2. [b] NICS values are calculated at points 1 Å above (on the same side as the methyls connected to the phenalenyl unit) and below (on the opposite side) the dummy atoms X_1−X_4.

In addition to the aromaticity criterion based on NMR chemical shifts, the NICS values are also used as indices of aromaticity.[30] For the RB3LYP and UB3LYP geometries of **11**, NICS values calculated at 1 Å above and below the dummy atoms X_1−X_4 (Chart 2) are tabulated in Table 4. The NICS values above and below dummy atoms X_1 and X_3 are on the same order of magnitude as those at the ring centers of **12**,[35b] and among the locations calculated, the NICS values of the smallest magnitude are found above and below dummy atom X_4, which is the center of the entire molecule. These negative values are indicative of aromaticity for both the RB3LYP geometry and the UB3LYP geometry of **11** (open-shell system).[39] Comparing the NICS values of the two geometries, we find that NICS values of the RB3LYP geometry are more negative, pointing once again to a higher degree of aromaticity for the RB3LYP geometry.

The calculated ^{1}H and ^{13}C NMR spectra of **14**$^{2-}$ are compared with experimental spectra[40] in Figures 7 and 8, respectively. As can be seen from Figures 7 and 8, the π-bonded C_{2h} structure has much better agreement with the experimental spectra than the σ-bonded C_2 structure, especially in terms of the methyl ^{1}H and the methyl ^{13}C signals. The π-bonded C_2 structure with distortion has twice as many signals as the π-bonded C_{2h} structure, but the fast exchange due to vibrations leads to pairwise coalescences, and finally the number of peaks will be the same as those of the C_{2h} structure. The experimental ^{13}C spectra exhibit seven lines in the sp^2 carbon region, indicating the absence of sp^3-hybridized carbons other than the four methyl carbons. These ^{1}H and ^{13}C NMR spectra indicate that the π-bonded structure is what has been observed for **14**$^{2-}$ experimentally. This analysis provides further indirect evidence for the reality of the π-intermediate **10** in the Cope rearrange-

(38) Lazzeretti, P. *Phys. Chem. Chem. Phys.* **2004**, *6*, 217.
(39) Gogonea, V.; Schleyer, P. v. R.; Schreiner, P. R. *Angew. Chem., Int. Ed.* **1998**, *37*, 1945.
(40) Rohrbach, W. D.; Gerson, F.; Möckel, R.; Boekelheide V. *J. Org. Chem.* **1984**, *49*, 4128.

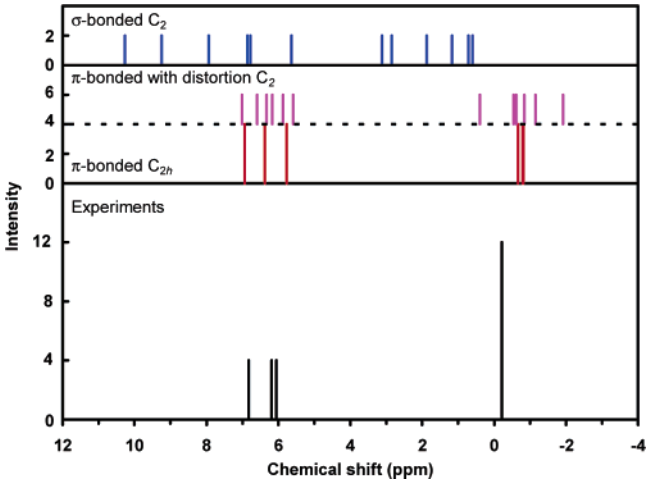

Figure 7. Experimental ^{1}H NMR spectrum of $\mathbf{14}^{2-}$ at 193.15 K at 360 Hz from ref 40, compared with those calculated from B3LYP/6-31G*. Chemical shift is relative to TMS.

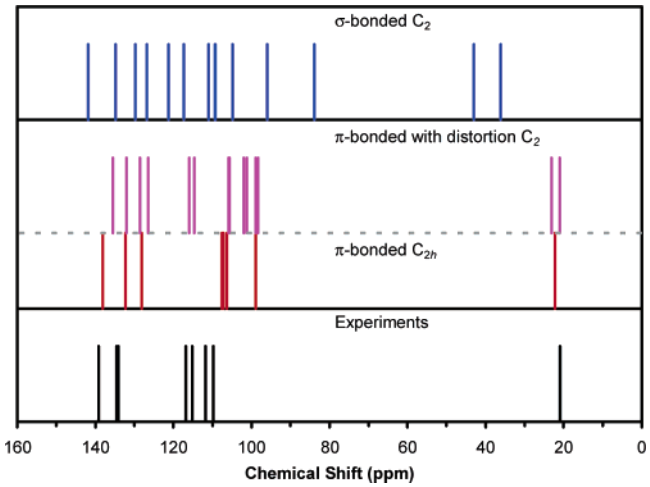

Figure 8. Experimental ^{13}C NMR spectrum of $\mathbf{14}^{2-}$ at 221.15 K at 90.7 Hz from ref 40, compared with those calculated from B3LYP/6-31G*. Chemical shift is relative to the value of TMS (189.7710 ppm) calculated by the same methodology. Peak intensities are not given.

ment of the title compound **9** and for the π-bonded **13** as its global minimum.

Magnetic Properties. As can be seen from Figures 1 and 4, the energy levels close to the ground state of **9** include the degenerate singlets of the reactant **9** and the product **9′**, the singlet of the π-intermediate **10**, and its low-lying triplet. Only the triplet will respond to a magnetic field. Similar to the Bleaney−Bowers equation and on the basis of van Vleck formula,[41] we can derive the equation

$$\chi T = \frac{2Ng^2\beta^2}{k[3 + \exp(-J_1/kT) + 2\exp(-J_2/kT)]}$$

where χ is the paramagnetic susceptibility, T is the temperature, N is Avogadro's number, g is the gyromagnetic factor, β is the electronic Bohr magneton, and k is the Boltzmann constant. Taking the triplet of **10** as the reference level, we have the energy difference between the singlet of **10** and the triplet as $J_1 = -7.682$ kcal/mol, and the energy difference between the

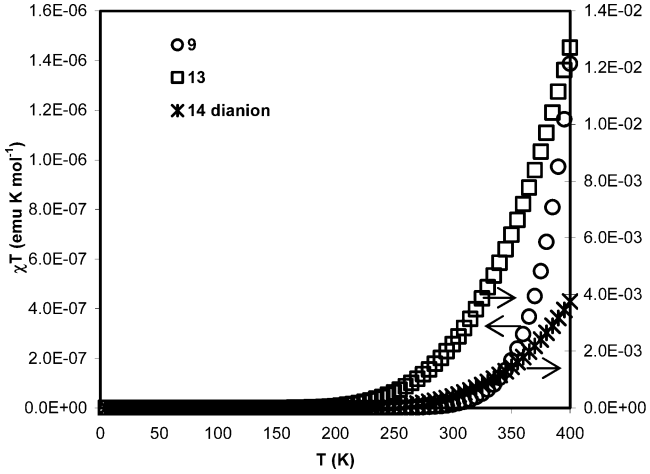

Figure 9. Calculated χT as a function of T for **9**, **13**, and $\mathbf{14}^{2-}$. The paramagnetic susceptibility signal comes from the triplet state of the π-bonded structures.

singlet of **9** or **9′** and the triplet as $J_2 = -11.038$ kcal/mol. The calculated χT as a function of T is shown in Figure 9. χT is on the order of 10^{-6} emu K mol^{-1} magnitude even at 400 K; therefore, the magnetic susceptibility of **9** is expected to be too low to be observed experimentally.

On the other hand, J_1 and J_2 for **13** are calculated as -4.274 and -1.690 kcal/mol, respectively, indicating that the π-bonded C_{2h} "intermediate" of **13** has a low-lying triplet and an energy lower than that of the σ-bonded C_2 "reactant". In this case, χT is estimated to be on the order of 10^{-3} emu K mol^{-1} magnitude at RT, which is comparable to that of the π-dimer of 2,5,8-tri-*tert*-butylphenalenyl (**8** in Scheme 3) measured by SQUID;[11b,42] therefore, **13** should have experimentally observable paramagnetism. In comparison, J_1 and J_2 for $\mathbf{14}^{2-}$ are calculated as -5.310 and 5.309 kcal/mol, respectively. Our estimated χT of $\mathbf{14}^{2-}$ becomes significant around RT, indicating a thermally accessible excited triplet state, which has been observed earlier by variable-temperature NMR spectra measured at 221.15 and 273.15 K.[40] This is again in concordance with our interpretation of a π-dimer structure of **13** and the π-intermediate of the title compound **9**.

Conclusions

In summary, we have found that the Cope rearrangement of cyclo-biphenalenyl **9** is stepwise, proceeding through an unusual π-intermediate **10** of C_{2h} symmetry which can be characterized as a $2\times13\pi+2\times2\pi$ system. The unusual π-intermediate has a long inter-phenalenyl distance of $R \approx 2.8$ Å, comparable to the intradimer C−C distance between two π-conjugated radicals in other π-dimers. The structure of the π-intermediate is unparalleled in the family of Cope rearrangements and cannot be anticipated on the basis of the Cope rearrangement of unsubstituted or substituted 1,5-hexadiene. This finding extends the previous Schreiner rule[7] in that the long-bonded intermediate is stabilized by a through-space multicenter covalent π-bonding interaction.

The energy of the π-intermediate **10** is higher than that of the global minimum **9** by ∼2 kcal/mol according to the employed RB3LYP hybrid DFT. NMR chemical shift calcula-

(41) Kahn, O. *Molecular Magnetism*; VCH Publishers: New York, 1993; pp 5−7, 104.

(42) The paramagnetism of **8** is also observable by ESR, see: Morita, Y.; et al. *Angew. Chem., Int. Ed.* **2002**, *41*, 1793.

tions support the σ-bonded **9** as the global minimum. A transition structure connecting the σ-bonded global minimum **9** and the π-bonded intermediate **10** has been identified. The calculated activation barrier of the Cope rearrangement of **9** is ~6 kcal/mol, consistent with the stepwise rearrangement mechanism whereby σ-bond breaking and multicenter π-bonding take place simultaneously.

Another minimum of C_{2h} symmetry is recognized as an aromatic intermediate, **11**, which can be characterized as a $26\pi+2\times2\sigma$ system with two σ-bonds between the two phenalenyl units and small bond length alternation plus extensive π-conjugation along the annulene-like molecular periphery. The aromatic character of this intermediate has been confirmed by ^{1}H NMR and NICS calculations. The energy of this aromatic intermediate lies at least 10 kcal/mol above the energy of the π-intermediate **10**, and therefore it does not contribute to the Cope rearrangement of **9**.

The shortening of inter-naphthalene distance in the π-bonded dianion and dication of cyclophane **14** indicates the presence of significant π-bonding interaction. Calculated ^{1}H and ^{13}C spectra of the π-bonded dianion of **14** agree with experiments. The analogy between $\mathbf{14}^{2-}$ and **10** provides indirect but strong evidence for the reality of the π-intermediate **10**. Further stabilization of the π-bonded structure through chemical modifications should allow such a π-bonded structure to be observed by X-ray diffraction and by paramagnetism for the ethano-bridged derivative **13**. These π-bonded structures offer us a paradigm for multicenter covalent π-bonding between π-conjugated radicals within one molecule. A good understanding of this multicenter π-bonding provides insights into the diverse properties of the phenalenyl radical family.[11,12,14−17,42−44]

Acknowledgment. Financial support from the National Science Foundation (Grant No. DMR-0331710) is gratefully acknowledged. We are indebted to Profs. Roald Hoffmann, Dean J. Tantillo, and Yves Rubin for their comments. We also thank Prof. Gyooson Park for discussions on NMR, and Prof. Michael Winokur for discussions on the X-ray structures of **9**. Discussions with Prof. Timothy H. Warren, Prof. K. Travis Holman, and Dr. Shuqiang Niu are also gratefully acknowledged. In addition, we thank the reviewers for their constructive and insightful comments.

Supporting Information Available: Complete refs 11a, 26, 42, and 44; calculated geometries of the π-bonded and σ-bonded **13** (Table 1S) and of neutral **14**, π-bonded $\mathbf{14}^{2+}$ and $\mathbf{14}^{2-}$, and σ-bonded $\mathbf{14}^{2-}$ (Table 2S); side views of the HOMOs of the intermediates **10** and **11** (Figure 1S); NMR spectra of **9** and **10** calculated from B3LYP/6-311+G(2d) (Figure 2S); optimized geometries (as Cartesian coordinates) of all calculated structures (Table 3S); and energies and vibrational frequencies of the stationary points of **9**, **13**, and **14** (Table 4S). This material is available free of charge via the Internet at http://pubs.acs.org.

JA060427R

(43) Huang, J.; Kertesz, M. *J. Am. Chem. Soc.* **2006**, *128*, 1418; **2003**, *125*, 13334.
(44) Kubo, T.; et al. *Angew. Chem., Int. Ed.* **2005**, *44*, 6564.